

Exploring the three-level Rabi problem with explicit numerical methods

Ben Burrill

CSUN Phys 451

December 2022

Abstract

Using a staggered-time explicit numerical method, I solved the time-dependent Schrödinger equation for a multi-level Rabi problem in the infinite square well. By producing a perturbation resonant between three energy levels, I induced flopping behavior. The numerical results were compared with theoretical predictions for the three-level Rabi problem using the rotating wave approximation.

1 Introduction and Methods

1.1 Solving the TDSE numerically

As an oscillatory, stiff partial differential equation, naïve application of the Euler method to the time-dependent Schrödinger equation rapidly leads to instability. However, explicit methods can still be used, so long as stability conditions are obeyed. I used a simple staggered-time algorithm described by Visscher [3]. Visscher writes the Schrödinger equation as a system of coupled equations of the real and imaginary parts of the wavefunction. This can be shown easily from the Schrödinger equation as follows:

$$\begin{aligned} i\hbar \frac{\partial}{\partial t} (\Psi_r + i\Psi_i) &= \hat{H} (\Psi_r + i\Psi_i) \\ \hbar \frac{\partial}{\partial t} (\Psi_r + i\Psi_i) &= \hat{H} (\Psi_i - i\Psi_r) \end{aligned}$$
$$\begin{cases} \hbar \frac{\partial \Psi_r}{\partial t} = \hat{H} \Psi_i \\ \hbar \frac{\partial \Psi_i}{\partial t} = -\hat{H} \Psi_r \end{cases} \quad (1)$$

Visscher notes the similarity of these coupled equations to those from second-order mechanics problems. Such problems are commonly solved using staggered-time explicit methods, and this can be done here as well. I think that it is also interesting to observe from this that if we were so inclined, we could even write the Schrödinger equation as a second-order real PDE, at least for time-independent Hamiltonians:

$$\begin{aligned} \hbar \frac{\partial^2 \Psi_r}{\partial t^2} &= \frac{\partial}{\partial t} (\hat{H} \Psi_i) = \hat{H} \left(-\frac{1}{\hbar} \hat{H} \Psi_r \right) \\ \hbar^2 \frac{\partial^2 \Psi_r}{\partial t^2} &= -\hat{H}^2 \Psi_r \end{aligned}$$

In any case, the actual numerical method is very straightforward. We define the real wavefunction at integer timesteps and the imaginary wavefunction at half-integer timesteps, and update both according to Equation 1. To highlight the simplicity of the algorithm, a simplified implementation of a time step is shown in Python (using $\hbar = 1$):

```
1 step += 1
2 R += dt * H(I, dt * (step-0.5))
3 I -= dt * H(R, dt * step)
```

We can then define the Hamiltonian (given here for 1D):

```
1 def H(f, t):
2     return V(t) * f - d2(f)/dx2_2m
3
4 def d2(f):
5     diff = -2 * f
6     diff[:-1] += f[1:] # f(x+dx)
7     diff[1:] += f[:-1] # f(x-dx)
8     diff[0] -= f[1]
9     diff[-1] -= f[-2]
10    return diff
```

Where $V(t)$ is the time-dependent potential for the system, R and I are `numpy` arrays for the real and imaginary parts of the wavefunction, dt is the timestep, and $dx2_2m = 2m(\Delta x)^2$.

Additionally, boundary conditions for the infinite square well may be imposed by forcing R and I to be 0 at their

boundaries.

1.2 Stability conditions

Visscher evaluated the stability conditions of the previously described staggered-time algorithm, and determined that stability is guaranteed under the condition:

$$-\frac{2}{\Delta t} \leq V \leq \frac{2}{\Delta t} - \frac{2}{m\Delta r^2}$$

As a practical matter, at least for my usage, V is rarely large enough to affect stability, so we can consider it to be 0 and rewrite the stability condition (using the variables from the Python code) as `dt <= min(dx2_2m)/2`.

These stability conditions are very strict, and must be observed with care, though if you do violate them you at least won't need to wait long to notice. For my purposes, I found that increasing `dt` beyond the stability threshold by any more than 0.01% would lead to almost immediate instability. However, so long as the stability conditions are met, I found the simulation to behave quite sensibly, even with relatively large timesteps.

1.3 A Rabi problem in the infinite well

In this work, we will be considering time-dependent oscillatory perturbations in the infinite square well. The perturbing field takes the form

$$V(t) = Ax \sum_k \sin(\omega_k t)$$

The problem bears strong resemblance to the Rabi problem. As typically formulated, the Rabi problem is conceived as a strictly two-level system, where as in our case countably infinite energy levels are reachable. The equations of motion for the coefficients of the unperturbed eigenstates, C_m can then be written as

$$\begin{aligned} \dot{C}_m &= -\frac{i}{\hbar} \sum_{n=1}^{\infty} \langle m | V(t) | n \rangle C_n e^{-i\omega_{mn}t} \\ &= -\frac{i}{\hbar} \sum_{n=1}^{\infty} V_{mn} C_n e^{-i\omega_{mn}t} \sum_k \sin(\omega_k t) \end{aligned} \quad (2)$$

Where $V_{mn} = \langle m | Ax | n \rangle$, which for the infinite square well, this is given by:

$$\begin{aligned} V_{mn} &= \frac{2}{a} \int_0^a \sin\left(\frac{n\pi x}{a}\right) \sin\left(\frac{m\pi x}{a}\right) Ax dx \\ &= \frac{2Aa^2}{\pi^2} \left(\frac{1}{(n-m)^2} - \frac{1}{(n+m)^2} \right) \end{aligned} \quad (3)$$

To simplify analysis, we will tune the ω_k frequencies to be the resonance frequencies between energy levels we are interested in, that is:

$$\omega_k = \omega_{mn} = \frac{E_m - E_n}{\hbar} = \frac{m^2 - n^2}{2\pi^2\hbar}$$

In principle, the resonant perturbations between two energy levels could also cause some temporary “leakage” of probability to any of the other infinitely many levels, and a careful Fourier analysis of Equation 2 might be able to quantify this effect. However, from what we do know about the two-level Rabi problem, the maximum transition probability P falls off rapidly with detuning:

$$P \propto \frac{1}{(\omega - \omega_0)^2}$$

So for the purposes of our theoretical analysis, we will assume that transitions are only permitted between pairs of levels which have a corresponding perturbation term in our Hamiltonian at the resonance frequency ω_{mn} .

1.4 The rotating wave approximation

Sargent and Horwitz [2], considered the case of three-level Rabi flopping, using the rotating wave approximation to solve for the coefficients of the unperturbed eigenstates as a function of time.

A good explanation of the rotating-wave approximation is

given by Fujii [1]. In the rotating wave approximation, we use the trigonometric identities of Euler, $2i \sin(\theta) = e^{i\theta} - e^{-i\theta}$, and neglect the counter-rotating term from the perturbing Hamiltonian, using either the positive or negative rotating term where needed such that the Hermiticity of the Hamiltonian is preserved. The overall effect of the approximation is that it removes rapidly oscillating terms.

Under the rotating wave approximation, we will rewrite the time-dependent sinusoidal perturbations for $n = 1$ to $n = 2$ and $n = 2$ to $n = 3$ transitions:

$$\sum_k \sin(\omega_k t) = \frac{\pm 1}{2i} \sum_k e^{\pm i\omega_k t} = \frac{\pm 1}{2i} (e^{\pm i\omega_{12}t} + e^{\pm i\omega_{23}t})$$

The \pm values in the above equation are for the Hermitian conjugate pairs.

Unlike Sargent and Horwitz, which considered the general case of non-zero detuning for both resonance frequencies, we only care about the case of resonant perturbations, which greatly simplifies the analysis, as it leaves us with just a system of homogeneous differential equations when we apply the rotating wave approximation and our other assumptions to Equation 2:

$$\begin{cases} \dot{C}_1 = \frac{-1}{2\hbar} V_{12} C_2 \\ \dot{C}_2 = \frac{-1}{2\hbar} (-V_{21} C_1 + V_{23} C_3) \\ \dot{C}_3 = \frac{1}{2\hbar} V_{32} C_2 \end{cases}$$

Rewriting into matrix form:

$$\dot{\mathbf{C}} = -\frac{1}{2\hbar} \begin{pmatrix} 0 & V_{12} & 0 \\ -V_{21} & 0 & V_{23} \\ 0 & -V_{32} & 0 \end{pmatrix} \mathbf{C}$$

Using $V_{nm} = V_{mn}$, the eigenvalues are $0, \pm \frac{i}{2\hbar} \sqrt{V_{12}^2 + V_{23}^2}$, and finding the corresponding eigenvectors we can write the solution as

$$\mathbf{C}(t) = \alpha_1 \begin{pmatrix} V_{23} \\ 0 \\ -V_{12} \end{pmatrix} + \alpha_2 \begin{pmatrix} V_{12} \\ V \\ V_{23} \end{pmatrix} e^{-\frac{iVt}{2\hbar}} + \alpha_3 \begin{pmatrix} V_{12} \\ -V \\ V_{23} \end{pmatrix} e^{\frac{iVt}{2\hbar}}$$

where $V = \sqrt{V_{12}^2 + V_{23}^2}$.

Using the initial conditions $|\Psi_0\rangle = |1\rangle$, we can find the squared modulus of each coefficient:

$$\begin{aligned} |C_1(t)|^2 &= \left(\frac{V_{23}^2}{V^2} + \frac{V_{12}^2}{V^2} \cos(Vt/2\hbar) \right)^2 \\ |C_2(t)|^2 &= \frac{V_{12}^2}{V^2} \sin^2(Vt/2\hbar) \\ |C_3(t)|^2 &= \frac{V_{12}^2 V_{23}^2}{V^4} (\cos(Vt/2\hbar) - 1)^2 \end{aligned} \quad (4)$$

This is equivalent to the result obtained by Sargent and Horwitz for the special case they showed in their paper.

Although it will not be a focus of this work (because I ran out of time), the nice thing about simplifying the problem so that it can be written as a homogeneous system is that the technique generalizes to Rabi problems with even more levels. In the case of a four-level system we obtain eigenvalues to the characteristic matrix of the form

$$\lambda = \pm \frac{i}{2\sqrt{2}\hbar} \sqrt{V^2 \pm \sqrt{V^4 - 4V_{12}^2 V_{34}^2}}$$

Where $V = \sqrt{V_{12}^2 + V_{23}^2 + V_{34}^2}$. This lets us get some idea about the oscillatory behavior of the system. It is interesting to note the role that $V = \sqrt{\sum_{n,m} V_{nm}^2}$ seems to play in determining the overall periodicity of the system.

2 Results and Discussion

Using the perturbing potential as described in Section 1.3 oscillating with a mix the resonance frequencies from $n = 1$ to 2 and $n = 2$ to 3, ie $V(t) = Ax(\sin(\omega_{12}t) + \sin(\omega_{23}t))$, I induced three-level flopping behavior in the numerical simulation. I used a timestep, $\mathbf{dt}=2 \times 10^{-5}$, and a uniform spatial

array such that $\text{dx}2.2\text{m}=\frac{2}{150}$.

The probabilities of finding the particle in each state, $|C_n|^2 = |\langle n | \Psi \rangle|^2$ were determined by integration with the trapezoidal rule on the numerical wavefunction. These are plotted in Figure 1. Also shown in the figure is the probability that the particle could be found in any other state, $P_{\text{other}} = 1 - |C_1|^2 - |C_2|^2 - |C_3|^2$. This was seen to remain nearly at zero over the course of the entire simulation, which is agreement with assumption we made in our theoretical analysis.

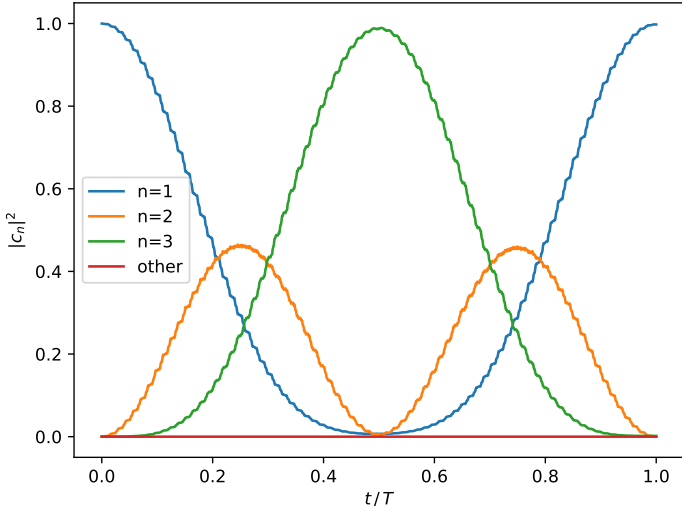


Figure 1: Numerical results of the multi-level infinite square well Rabi problem with a resonant perturbation between three states

The theoretical predictions from Equation 4 are plotted in Figure 2. The overall shape is in very good agreement with the simulation, although the simulation clearly has a high-frequency oscillation that is not accounted for by the theoretical predictions. This is not surprising because the elimination of rapidly oscillating terms is central to the rotating wave approximation. Because of this, it seems reasonable to assume that these oscillations are not due to numerical error, and are simply due to the approximations made in our theoretical analysis, and might have been able to be predicted by a higher order perturbation theory.

To better evaluate the discrepancy between simulation and

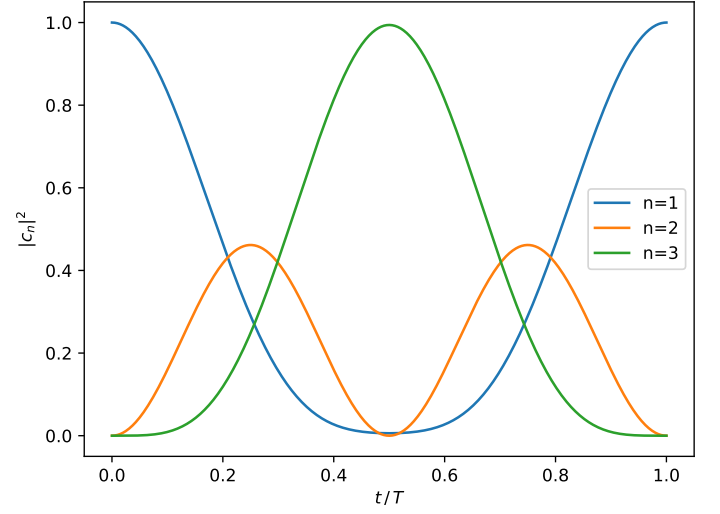


Figure 2: Theoretical prediction of the three-level Rabi problem under the rotating-wave approximation

theory, the residuals, $|C_{n,\text{simulated}}|^2 - |C_{n,\text{theory}}|^2$ are plotted in Figure 3. The standard deviation from the predicted probabilities is 4.8×10^{-3} .

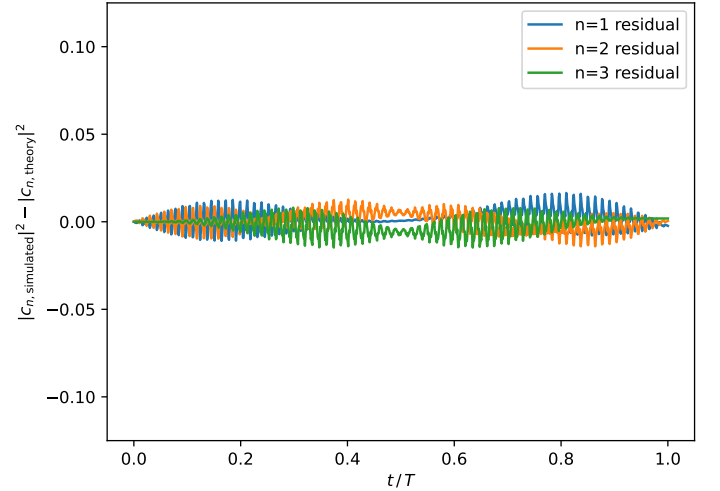


Figure 3: Residuals between the numerical and theoretical results. To better show detail, the range of the vertical axis is 1/4 that of Figure 1.

To determine the frequency of the periodic deviations, a frequency spectrum was produced and shown in Figure 4. This reveals that the high-frequency oscillations seen in Figure 1 are related to the driving frequencies, with the largest high-frequency peaks in the residual spectrum are at ω_{12} , ω_{23} , and $\frac{\omega_{12} + \omega_{23}}{2}$.

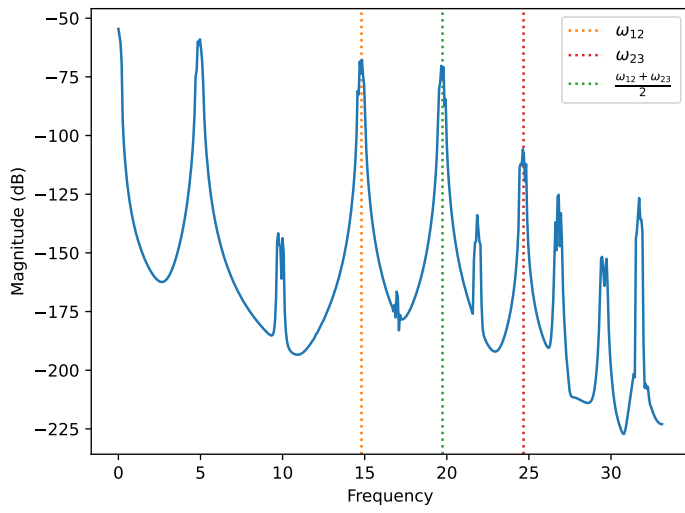


Figure 4: Spectrum plot of the residuals for $n=1$, with the driving frequencies (and their average) highlighted

3 Conclusions

I explored three-level Rabi flopping in the infinite square well using an explicit staggered-time numerical method, obtaining good correspondence with theoretical predictions for a three-level system under the rotating-wave approximation.

High frequency oscillations were found in the numerical simulation, at frequencies related to the driving frequency, that are not accounted for by the theoretical predictions. This is to be expected for the rotating-wave approximation used to produce the theoretical predictions and is not perceived to be due to numerical error.

The speed and simplicity of the staggered-time algorithm described by Visscher are very advantageous for quickly exploring and gaining intuition about simple quantum systems, with real-time animation of one-dimensional quantum systems easily accomplished using the `matplotlib` package. In 1991, Visscher noted that the algorithm brought the “time [to perform a simulation] down to the order of magnitude of a typical student attention span”, and thanks to advances in computer technology since then, I can attest that it has managed to remain at that level.

References

- [1] Kazuyuki Fujii. Introduction to the rotating wave approximation (rwa): Two coherent oscillations. *Journal of Modern Physics*, 8(12):2042–2058, 2017.
- [2] Murray Sargent III and Paul Horwitz. Three-level Rabi flopping. *Physical Review A*, 13(5):1962, 1976.
- [3] PB Visscher. A fast explicit algorithm for the time-dependent Schrödinger equation. *Computers in Physics*, 5(6):596–598, 1991.